Asian Journal of Chemistry; Vol. 30, No. 7 (2018), 1564-1568

ASIAN JOURNAL OF CHEMISTRY

https://doi.org/10.14233/ajchem.2018.21244

Preparation of Graphene Oxide/Bacterial Cellulose Nanocomposite *via in situ* Process in Agitated Culture

S.A. AMATURRAHIM, S. GEA*, D.Y. NASUTION and Y.A. HUTAPEA

Department of Chemistry, Faculty of Mathematic and Natural Sciences, University of Sumatera Utara, Medan 20155, Indonesia

*Corresponding author: Fax: +62 61 8214290; Tel: +62 61 8211050; E-mail: s.gea@usu.ac.id

Received: 20 January 2018; *Accepted*: 27 February 2018; *Published online*: 31 May 2018; AJC-18931

Graphene oxide/bacterial cellulose (GO/BC) nanocomposite has been successfully carried out with *in situ* process in agitated culture. During the *in situ* process, graphene oxide was partially reduced. Interaction between bacterial cellulose and graphene oxide was investigated by FTIR. The addition of graphene oxide improved the thermal and mechanical properties of nanocomposite. This is indicated by increasing residual mass from 29.41 % of GO/BC 0.04 wt % to 33.91 % of GO/BC 0.1 wt %. When compared to pristine bacterial cellulose, GO/BC 0.1 wt % nanocomposite increased in tensile strength from 50.5 MPa to 102.7 MPa and Young's modulus from 2.0 GPa to 8.3 GPa. The morphology of nanocomposite films is presented that graphene oxide is well dispersed in the network of bacterial cellulose, but the agitation method is significantly enlarged the pores between fibril and also minimized the sizes of fibril, in which the average size of bacterial cellulose fibril dan pores are 68 nm and 440 nm, respectively.

Keywords: Bacterial cellulose, Graphene oxide, Nanocomposite, *in situ* Process, Agitated culture.

INTRODUCTION

Graphene oxide (GO) is a precursor in graphene synthesis has been widely used as a reinforcing material in various composite polymers. The reinforced nanocomposite polymers containing nano-sized carbon substances such as carbon nanotubes (CNTs) and graphene have been studied intensively in recent years [1]. Graphene and its derivatives have been used to form nanocomposites with various polymeric materials such as poly(vinyl alcohol) [2], chitosan [3], polyacrylamide [4], epoxy [5], poly (sodium acrylate) [6] and nanocellulose [7].

Bacterial cellulose (BC) has a unique physical and chemical properties that are different from plants cellulose such as high tensile strength, high water holding capacity, high crystallinity, fine fibers, good fiber network structure, transparent, fiber binding ability, bio-campatible, biodegradation and moldability [8-11]. The size of graphene oxide single layer thickness is experimentally estimated to be 1 nm approximately [12].

Although the mechanical strength of graphene oxide was reported to be lower than graphene, it has large Young Modulus (207.06 GPa) [13]. Graphene oxide is an insulator with Rs of 10-12 Ω/Sq due to the interference of the electron π delocalization which is conjugated with the C-O sp^3 bond [14]. Since graphene oxide is easily dispersed in organic solvents, water and matrix sharing due to the presence of a functional group containing oxygen, it gives an advantage to mix graphene oxide with a polymeric material to improve its electrical, mechanical and thermal properties. Moreover, as the number of hydroxyl groups in bacterial cellulose is larger, the effective interaction between bacterial cellulose and graphene oxide, electrostatic interactions and hydrogen bonds are potentially achievable [15].

The research reported the preparation of graphene derivation-based nanocomposite (graphene oxide) and bacterial cellulose by *ex situ* method [16]. The results showed that the *ex situ* method produced nanocomposites with bacterial cellulosic structures that have been damaged in 3D and the interaction between layers of graphene oxide easily produced an agglomeration in the matrix. Preparation of poly(vinyl alcohol) (PVA)/bacterial cellulose *in situ* produces composites with better mechanical and optical properties due to more effective and homogeneous mixing of components [17]. The preparation of bacterial cellulose/Mater-Bi bionanocomposite showed a significant increase in thermal and mechanical properties with the addition of bacterial cellulose to Mater-Bi [18]. Moreover, the preparation of GO/BC nanocomposites *in situ* with static culture media showed a decreasing degrees of crystallinity of bacterial cellulose and some graphene oxide are reduced during the biosynthesis process. Finally, the presence of graphene oxide can increase tensile strength and modulus compared to pure bacterial cellulose due to disperse uniformity and interaction between graphene oxide and bacterial cellulose [15].

To sum up, the researcher is interested to conduct a research to prepare GO/BC nanocomposite *via in situ* with agitation culture media. This research is intended to ensure the uniformity of the spread of graphene oxide in the cellulose matrix of bacteria without damaging its nanocomposite structre and to enchance its mechanical and thermal properties.

EXPERIMENTAL

Graphite, H_2SO_4, $NaNO_3$, $KMnO_4$, H_2O_2, NaOH, CH_3COOH, sucrose and urea were purchased from Aldrich Merck Sigma. Coconut water was purchased from Medan traditional market. The bacterial strain of *Acetobacter xylinum* was obtained from Microbiology Laboratorium, University of Sumatera Utara. Graphene oxide was prepared *via* a modified Hummers Method through an acid oxidation towards the graphite [14-19].

General procedure: GO/BC nanocomposite was made with the help of the bacterial strain of *Acetobacter xylinum*. The culture medium was consisted of 50 mL coconut water, 0.5 g of urea, 0.25 g of sucrose and addition of CH_3COOH to reach the pH of 4.5.

Graphene oxide 1 % (w/v) colloidal suspension with variations of 2, 4 and 6 mL in volumes were added to the culture medium and autoclaved for 15 min at 121 °C. Then, it was stirred for 30 min and continued to ultrasonification process for 1 h to improve the dispersed graphene oxide in culture media. After that, the solution was autoclaved for 5 min to eliminate the possible contaminants. After the culture medium reached room temperature, as many as 5 mL of *Acetobacter xylinum* bacteria was inoculated in incubator at 28 °C for 7 days at a speed of 100 rpm. Then, GO/BC nanocomposite was soaked with 2.5 % NaOH for 1 night, washed with aquadest to reach neutral pH. Furthermore, GO/BC nanocomposite was pressed using a hot-press with wire mesh at 115 °C for 10 min. Finally, it was characterized by SEM, TGA, FTIR and tensile strength test. The resulted GO/BC nanocomposites possessed a graphene oxide levels of 0.04, 0.07 and 0.1 wt %, respectively.

Detection method: The GO/BC nanocomposites were characterized by scanning electron microscope (SEM EDX EVO MA 10 carl Zeiss Bruker operating at 20 kV). Samples were recorded at a magnification between 1000 to 10000x their original sizes. Fourier transform infrared (FTIR) spectra were recorded with Shimadzu IR Prestige-21 spectrometer with a disc of KBr. All FTIR spectra were recorded in the transmittance mode in the range of 4000-400 cm^{-1}. Thermogravimetric analysis (TGA) was carried out by using TGA SDT Q600 V20. The samples were heated from 35-600 °C with heating rate of 10 °C/min under nitrogen atmosphere. X-ray diffraction (XRD) pattern were taken by Shimadzu XRD-6100 diffractometer using Cu-K_α radiation ($\lambda = 0.154$ nm) at scanning rate of 2 °/min, a voltage of 40 kV and a current of 200 mA. The diffraction angle (2θ) range from 5° to 30° with a step size of 0.02°. Tensile strength test were performed on a tensile strength machine graphene oxideTECH AL 7000 M with a 1 kN static load cell. The rectangular specimen (40 mm × 10 mm × ~1 mm) were used for tensile tests under ambient conditions (with humidity 65 %) and at a speed of 1 mm/min. All measurements were performed for at least three samples and the average value was recorded.

RESULTS AND DISCUSSION

X-ray diffraction analysis: The XRD patterns of graphite and graphene oxide are shown in Fig. 1. The characteristic 2θ of graphite was appeared at 26.369° with d-spacing of 3.37721 Å [20]. Afteroxidation process, thepeak shifts to 2θ = 9.0715° with d-spacing of 9.74063 Å which indicatedthat graphene oxide has been formed. A broad peak caused by the oxygen rich groups (-OH, C-O-C, C=O) and water molecules trapped on both sides of the sheets of graphene oxide [21].

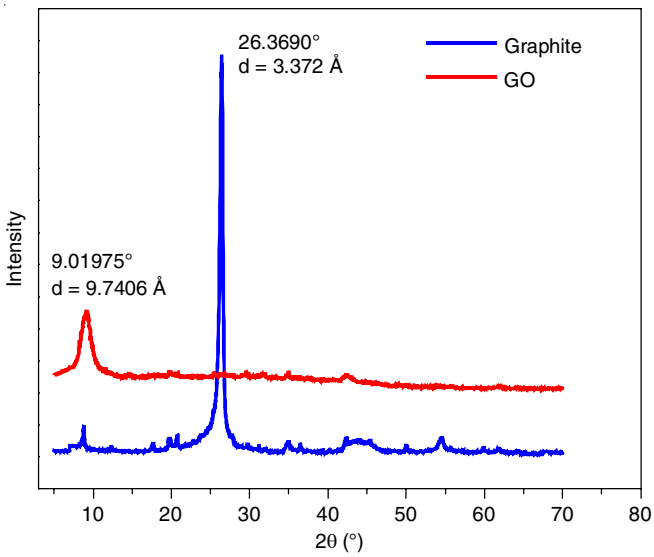

Fig. 1. XRD pattern of graphite and grapheme oxide

FTIR analysis: The FTIR spectra of graphite, graphene oxide, bacterial cellulose, GO/BC nanocomposites are displayed in Fig. 2. The characterization by FTIR was performed to confirm the changes of functional group before and after oxidation process in graphene oxide preparation and also to confirm the interaction that occur between graphene oxide and bacterial cellulose as a component in nanocomposite. In case of the graphite, the FTIR spectrum was typical and the domi-

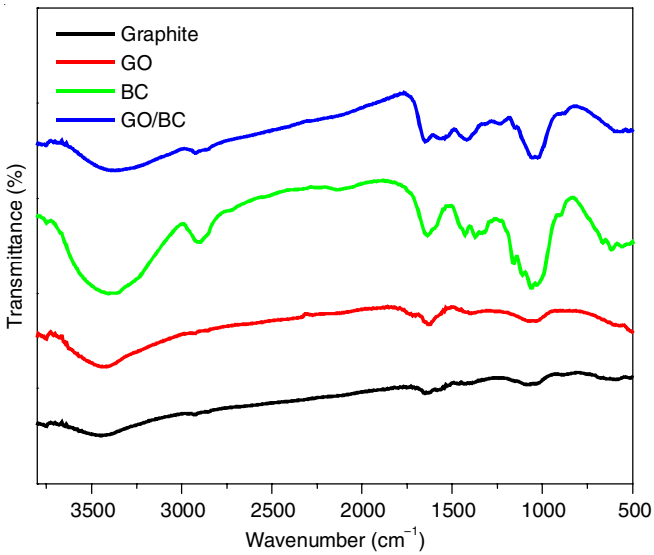

Fig. 2. FTIR spectra of graphite, grapheme oxide, bacterial cellulose, grapheme oxide/bacterial cellulose (GO/BC) nanocomposites

nating signal was at 1635 cm^{-1}, corresponding to the skeletal vibration of aromatic C=C bond [22].

The broad and intense peak at 3425 $cm^{-1}$of graphene oxide is assigned as the O-H stretching vibrations and the peak at 1720 cm^{-1} corresponded to the stretching vibrations of C=O carboxylic moieties. The intense peak at 1627 cm^{-1} was attributed to skeletal vibration of aromatic C=C bond or the deformation vibrations of the O-H band of intercalated water molecules [23]. Other peaks at 1396, 1203 and 1050 cm^{-1} can be attributed to the deformation vibration of tertiary alcohol C-OH, the epoxy C-O stretching vibration and the alkoxy C-O stretching vibration, respectively [24].

In the spectrum of bacterial cellulose, the dominating signal was at 3410 cm^{-1}, corresponding to the intermolecular hydrogen bond for 3O···H–O5 [25]. In the stretching vibration region, the peak at 1157, 1111, 1061 and 1033 cm^{-1} are assigned to the asymmetric bridge stretching of C1-O-C4, C2-O2H, C1-O-C5 pyranose ring skeletal stretching and C6H2-O6H, respectively [26]. The peak at 1427 cm^{-1} corresponds to bending of HCH, HCO and the intense peak at 1635 cm^{-1} attributed to –OH of water molecules trapped on network of bacterial cellulose [25].

The characteristic vibrations in the spectra of GO/BC nanocomposites are same as bacterial cellulose with small difference. Compared with spectrum of graphene oxide, the disappearance of the peak of C=O at 1720 cm^{-1} in nanocomposites spectra indicated that graphene oxide was partially reduced during the biosynthesis process [23]. The broadened peak at 3371 cm^{-1} and the relative intensity changes of the C-O stretching vibration in GO/BC nanocomposites implied the hydrogen bonds in bacterial cellulose were disturbed. Effective interaction such as hydrogen bonding between the oxygen group on graphene oxide and the hydroxyl groups in the bacterial cellulose unit is potentially achievable [16]. This is indicated by decreasing absorption of stretching vibration of C-O epoxy, C-O alkoxy and bending OH to 1234, 1026 and 1419 cm^{-1}, respectively [23].

Mechanical properties: To evaluate the reinforcing effect of graphene oxide in GO/BC nanocomposites, tensile strength test of pure bacterial cellulose and three GO/BC film with a graphene oxide content of 0.04, 0.07 and 0.1 wt %, respectively was conducted. The representative stress-strain curves are shown in Fig. 3 and mechanical properties of the film are summarized in Table-1. Tensile strength of bacterial cellulose from agitation process was significantly decreased comparing bacterial cellulose from static process. The agitation process caused a decreasing of the hydrogen bond between the fibrils and affected the length of fibrils formed. Decreasing of hydrogen bonds lead to lower the crystallinity index so that tensile strength of bacterial cellulose was also decreased [27].

Mechanical properties of the GO/BC nanocomposite films are not only depend on fibril modulus but also interaction between bacterial cellulose and graphene oxide. Mechanical properties of GO/BC nanocomposites have improved with the increasing of graphene oxide loadings. Incorporation of 0.1 wt %, graphene oxide dramatically improved the mechanical properties of bacterial cellulose. Young Modulus and tensile strength of the GO/BC nanocomposites with 0.1 wt % graphene

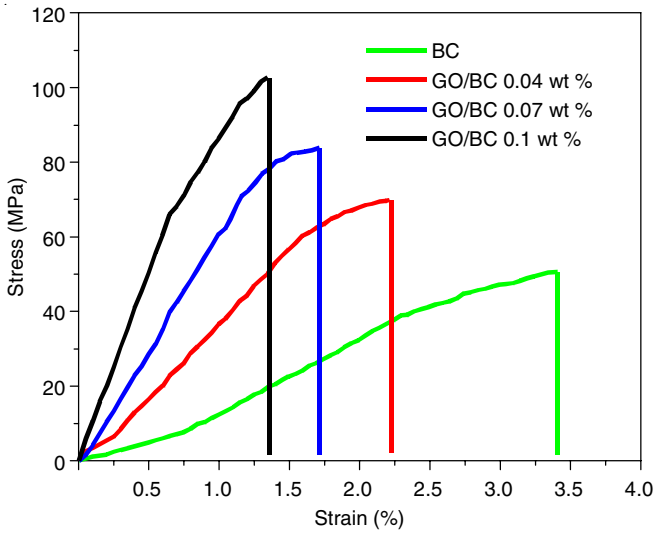

Fig. 3. Stress-strain curves of grapheme oxide/bacterial cellulose (GO/BC) nanocomposite films with a grapheme oxide content of 0.04, 0.07 and 0.1 wt %

TABLE-1
MECHANICAL PROPERTIES OF BACTERIAL CELLULOSE AND GRAPHENE OXIDE/ BACTERIAL CELLULOSE (GO/BC) NANOCOMPOSITE FILMS WITH DIFFERENT GRAPHENE OXIDE CONTENTS

Sample	Young Modulus (GPa)	Tensile strength (MPa)	Elongation at break (%)
Bacterial cellulose	2.0	50.5	3.43
GO/BC 0.04 wt %	4.8	69.9	2.21
GO/BC 0.07 wt %	6.3	83.8	1.71
GO/BC 0.10 wt %	8.3	102.7	1.34

oxide were measured to be 8.3 GPa and 102.7 MPa respectively. The improvement of 76 and 30 % higher than pure bacterial cellulose film, indicating that dispersion of graphene oxide nanosheet on the molecular scale in bacterial cellulose matix and also the interaction between graphene oxide and bacterial cellulose made a great contribution to the mechanical enhancement. The oxygen containing groups on graphene oxide can interact with OH on bacterial cellulose through hydrogen bonding both intra and intermolecularly. The elongation at break decreased from 3.43 % (bacterial cellulose) to 1.34 % (bacterial cellulose/0.1 wt %) due to the brittle nature of the graphene oxide nanosheet.

Thermal properties: Thermogravimetric curves of GO/BC film with a graphene oxide content of 0.04, 0.07 and 0.1 wt % are shown in Fig. 4. Also, the corresponding data are listed in Table-2. Thermogravimetric analysis can be used to characterize any material based on the measurement of weight change by increasing temperature and to detect the phase change due to a decomposition processes. The three samples of GO/BC films showed almost the same curve with three stages of weight loss. The initial weight loss occurred around 50-110 °C, which was attributed to water evaporation. Physically absorbed and hydrogen bond linked water molecules were lost at this first stages [28]. The second weight loss occurred between 110-350 °C can be assigned to the thermal degradation and decomposition of bacterial cellulose, which involved the formation of levo-glucose, *trans*-glycosylation and free radical reaction,

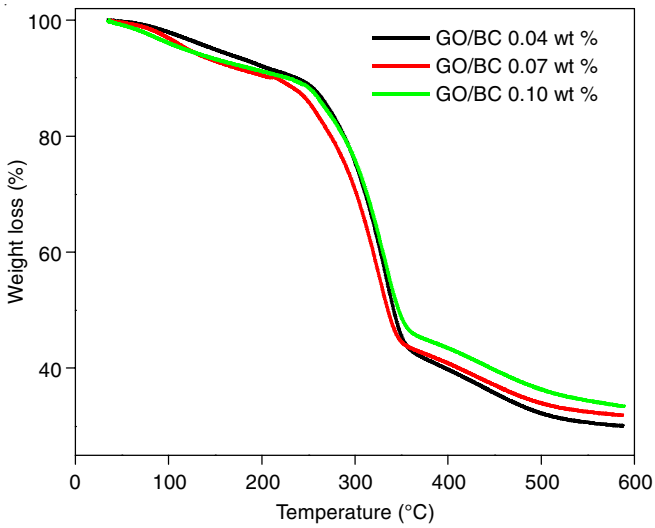

Fig. 4. TGA curves of grapheme oxide/bacterial cellulose (GO/BC) film with a grapheme oxide content of 0.04, 0.07 and 0.1 wt %

TABLE-2
RESIDUAL MASS (%) AND T_{max} (°C) OF GRAPHENE OXIDE/ BACTERIAL CELLULOSE (GO/BC) NANOCOMPOSITE FILMS WITH DIFFERENT GRAPHENE OXIDE CONTENTS

Sample	Residual Mass (%)	T_{max} (°C)
GO/BC 0.04 wt %	29.41	350.6
GO/BC 0.07 wt %	31.75	348.7
GO/BC 0.10 wt %	33.19	351.0

followed by generation of C, CO, CO_2, H_2O and combustible volatiles [29]. The decomposition temperature of graphene oxide was around 310 °C, which was related to the decomposition of the oxygen functional groups in graphene oxide [30]. The third weight loss occurred around 350-600 °C, which was attributed to carbonization process of GO/BC nanocomposite films. The increasing of graphene oxide concentration improved the thermal degradation resistance of GO/BC nanocomposites film which was characterized by the increasing of residual mass from 29.41 % for GO/BC 0.04 wt % to 33.19 % for GO/BC 0.1 wt %.

Morphology of GO/BC nanocomposites: SEM was performed to investigate the surface morphology of GO/BC nanocomposite films with magnification between 1000 and 10000x (Fig. 5). It indicated that graphene oxide nanosheet were dispersed uniformly within the bacterial cellulose matrix. The continuous agitation caused the cellulose fibrils and graphene oxide entangled with each other and created a more compact structure of GO/BC nanocomposites. Fig. 5c-d showed the bacterial cellulose morphology consisting of an ultrafine network structure made of random assembly of ribbon-shaped cellulose fibrils. The agitation method was significantly enlarged the pores between fibril and also minimized the sizes of fibril [31], in which the average size of bacterial cellulose fibril dan pores are 68 and 440 nm, respectively. The strong adhesion between graphene oxide nanosheet and bacterial cellulose

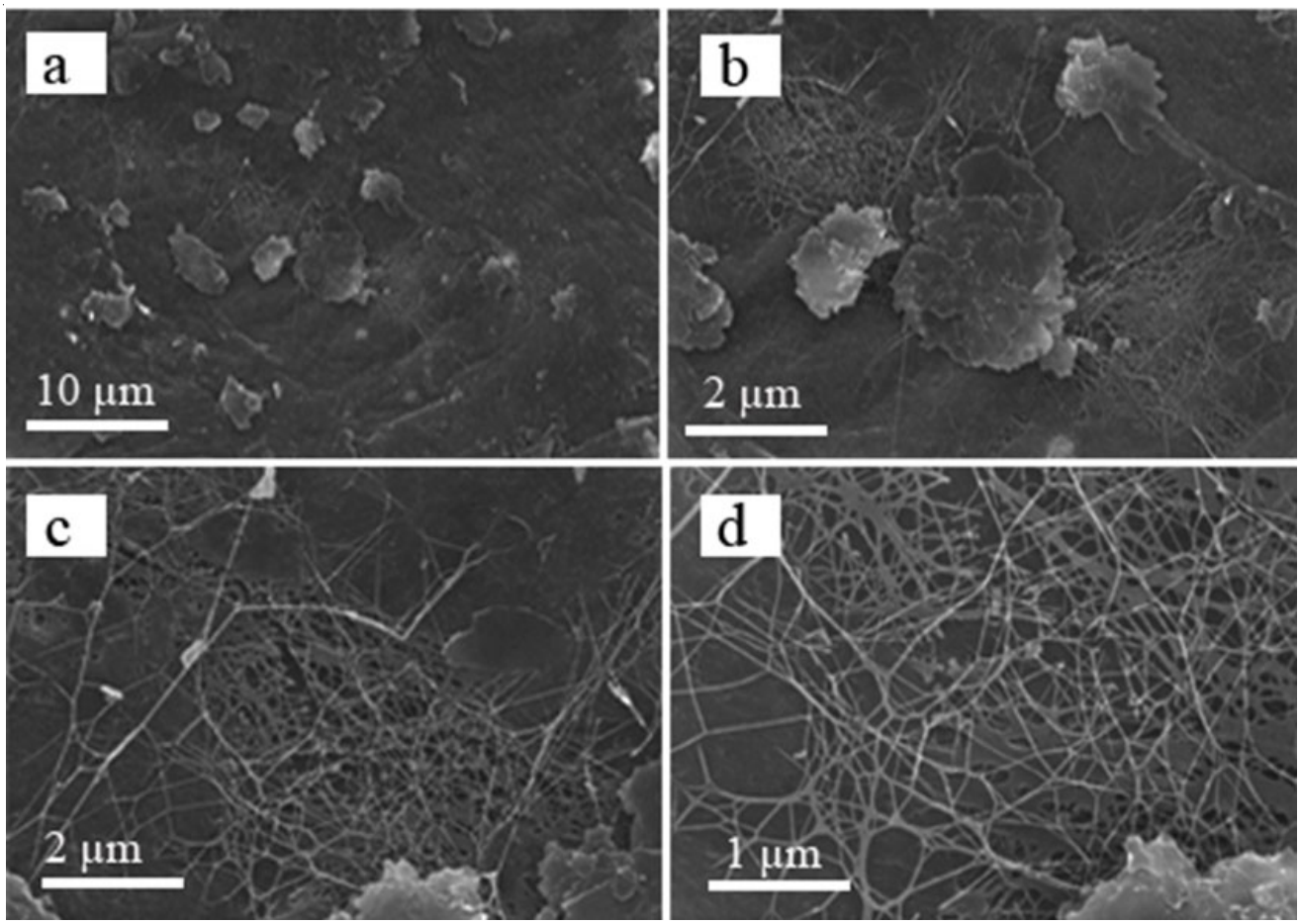

Fig. 5. SEM images of grapheme oxide/bacterial cellulose (GO/BC) nanocomposites with magnitude (a) 1000x, (b) 2500x, (c) 5000x and (d) 10000x

fibrils was beneficial to improve the mechanical properties of GO/BC nanocomposites. Fig. 6 shows the optical photograph film of bacterial cellulose (a), GO/BC 0.04 % wt (b), GO/BC 0.07 % wt (c), GO/BC 0.1 % wt (d).

Fig. 6. Film of bacterial cellulose (a), grapheme oxide/bacterial cellulose (GO/BC) 0.04 % wt (b), GO/BC 0.07 % wt (c), GO/BC 0.1 % wt (d)

Conclusion

In this work, graphene oxide/bacterial cellulose (GO/BC) nanocomposite was prepared by *in situ* process in agitated culture. During *in situ* process, graphene oxide was partially reduced because yeast extract containing many amino acid, which is ideal as reducing agent. The characterization by FTIR, SEM and TGA confirmed the existences of graphene oxide nanosheet in bacterial cellulose matrix. The integration of 0.1 wt % graphene oxide resulted in 76 % and 30 % increased in Young Modulus and tensile strength of the GO/BC nanocomposite films compared with pure bacterial cellulose. The interactions between graphene oxide and bacterial cellulose such as hydrogen bonding and the unidirectional uniform dispersion of graphene oxide nanosheet in bacterial cellulose matrix play important roles in the mechanical properties.

ACKNOWLEDGEMENTS

The authors acknowledge to Rector of University of Sumatera Utara for funding support through TALENTA 2018 *via* Basic Research Funding Scheme.

REFERENCES

1. J.N. Coleman, U. Khan and Y.K. Gun'ko, *Adv. Mater.*, **18**, 689 (2006); https://doi.org/10.1002/adma.200501851.
2. R. Liu, S. Liang, X.Z. Tang, D. Yan, X. Li and Z.Z. Yu, *J. Mater. Chem.*, **22**, 14160 (2012); https://doi.org/10.1039/c2jm32541a.
3. S. Ye, J. Feng and P. Wu, *J. Mater. Chem. A Mater. Energy Sustain.*, **1**, 3495 (2013); https://doi.org/10.1039/c2ta01142e.
4. H.W. Liu, S.H. Hu, Y.-W. Chen and S.-Y. Chen, *J. Mater. Chem.*, **22**, 17311 (2012); https://doi.org/10.1039/c2jm32772d.
5. S. Ye, J. Feng and P. Wu, *J. Mater. Chem.*, **1**, 3495 (2013); https://doi.org/10.1039/c2ta01142e.
6. Y. Zeng, L. Qiu, K. Wang, J. Yao, D. Li, G.P. Simon, R. Wang and H. Wang, *RSC Adv.*, **3**, 887 (2013); https://doi.org/10.1039/C2RA22173J.
7. J.M. Malho, P. Laaksonen, A. Walther, O. Ikkala and M.B. Linder, *Biomacromolecules*, **13**, 1093 (2012); https://doi.org/10.1021/bm2018189.
8. M. Ishihara, M. Matsunaga, N. Hayashi and V. Tisler, *Enzyme Microb. Technol.*, **31**, 986 (2002); https://doi.org/10.1016/S0141-0229(02)00215-6.
9. D. Klemm, D. Schumann, U. Udhardt and S. Marsch, *Prog. Polym. Sci.*, **26**, 1561 (2001); https://doi.org/10.1016/S0079-6700(01)00021-1.
10. O. Shezad, S. Khan, T. Khan and J.K. Park, *Korean J. Chem. Eng.*, **26**, 1689 (2009); https://doi.org/10.1007/s11814-009-0232-5.
11. E.J. Vandamme, S. De Baets, A. Vanbaelen, K. Joris and P. De Wulf, *Polym. Degrad. Stab.*, **59**, 93 (1998); https://doi.org/10.1016/S0141-3910(97)00185-7.
12. L.J. Cote, F. Kim and J. Huang, *J. Am. Chem. Soc.*, **131**, 1043 (2009); https://doi.org/10.1021/ja806262m.
13. J.W. Suk, R.D. Piner, J. An and R.S. Ruoff, *ACS Nano*, **4**, 6557 (2010); https://doi.org/10.1021/nn101781v.
14. J. Becerril, Z. Mao, R.M. Liu, Z. Stoltenberg, Y. Bao and Y. Chen, *ACS Nano*, **2**, 463 (2008); https://doi.org/10.1021/nn700375n.
15. H. Si, H. Luo, G. Xiong, Z. Yang, S.R. Raman, *Macromol. Rapid Commun.*, **35**, 1706 (2014); https://doi.org/10.1002/marc.201400239.
16. Y. Feng, X. Zhang, Y. Shen, K. Yoshino and W. Feng, *Carbohydr. Polym.*, **87**, 644 (2012); https://doi.org/10.1016/j.carbpol.2011.08.039.
17. S. Gea, E. Bilotti, C. Reynolds, N. Soykeabkeaw and T. Peijs, *Mater. Lett.*, **64**, 901 (2010); https://doi.org/10.1016/j.matlet.2010.01.042.
18. H. Nainggolan, S. Gea, E. Bilotti, T. Peijs and S.D. Hutagalung, *Beilstein J. Nanotechnol.*, **4**, 325 (2013); https://doi.org/10.3762/bjnano.4.37.
19. W.S. Hummers Jr. and R.E. Offeman, *J. Am. Chem. Soc.*, **80**, 1339 (1958); https://doi.org/10.1021/ja01539a017.
20. G. Shao, Y. Lu, F. Wu, C. Yang, F. Zeng and Q. Wu, *J. Mater. Sci.*, **47**, 4400 (2012); https://doi.org/10.1007/s10853-012-6294-5.
21. A.B. Bourlinos, D. Gournis, D. Petridis, T. Szabo, A. Szeri and I. Dekany, *Langmuir*, **19**, 6050 (2003); https://doi.org/10.1021/la026525h.
22. R.M. Silverstein, G.C. Basser and T.C. Masrill, Spectrometric Identification of Organic Compound, John Wiley & Sons, Inc., New York, edn 5 (1991).
23. S. Park, K.S. Lee, G. Bozoklu, W. Cai, S.T.T. Nguyen and R.S. Ruoff, *ACS Nano*, **2**, 572 (2008); https://doi.org/10.1021/nn700349a.
24. A.G. Nandgaonkar, Q. Wang, K. Fu, W.E. Krause, Q. Wei, R. Gorga and L.A. Lucia, *Green Chem.*, **16**, 3195 (2014); https://doi.org/10.1039/C4GC00264D.
25. S.Y. Oh, D. Yoo, Y. Shin, H.C. Kim, H.Y. Kim, Y.S. Chung, W.H. Park and J.H. Youk, *Carbohydr. Res.*, **340**, 2376 (2005); https://doi.org/10.1016/j.carres.2005.08.007.
26. N.I. Kovtyukhova, P.J. Ollivier, B.R. Martin, T.E. Mallouk, S.A. Chizhik, E.V. Buzaneva and A.D. Gorchinskiy, *Chem. Mater.*, **11**, 771 (1999); https://doi.org/10.1021/cm981085u.
27. S.H. Moon, J.M. Park, H.-Y. Chun and S.-J. Kim, *Biotechnol. Bioprocess Eng.*; *BBE*, **11**, 26 (2006); https://doi.org/10.1007/BF02931864.
28. W. Hu, S. Chen, B. Zhou and H. Wang, *Mater. Sci. Eng. B*, **170**, 88 (2010); https://doi.org/10.1016/j.mseb.2010.02.034.
29. W. Shao, H. Liu, X. Liu, S. Wang and R. Zhang, *RSC Adv.*, **5**, 4795 (2015); https://doi.org/10.1039/C4RA13057J.
30. Z. Yan, S. Chen, H. Wang, B. Wang and J. Jiang, *Carbohydr. Polym.*, **74**, 659 (2008); https://doi.org/10.1016/j.carbpol.2008.04.028.
31. S. Jeon, Y.M. Yoo, J.W. Park, H.J. Kim and J. Hyun, *Curr. Appl. Phys.*, **14**, 1621 (2014); https://doi.org/10.1016/j.cap.2014.07.010.